Atomic layer deposition of absorbing thin films on nanostructured electrodes for short-wavelength infrared photosensing

Jixian Xu, Brandon R. Sutherland, Sjoerd Hoogland, Fengjia Fan, Sachin Kinge, and Edward H. Sargent

Citation: Applied Physics Letters **107**, 153105 (2015); doi: 10.1063/1.4933380
View online: http://dx.doi.org/10.1063/1.4933380
View Table of Contents: http://scitation.aip.org/content/aip/journal/apl/107/15?ver=pdfcov
Published by the AIP Publishing

Atomic layer deposition of absorbing thin films on nanostructured electrodes for short-wavelength infrared photosensing

Jixian Xu,[1,a)] Brandon R. Sutherland,[1,a)] Sjoerd Hoogland,[1] Fengjia Fan,[1] Sachin Kinge,[2] and Edward H. Sargent[1,b)]
[1]*Department of Electrical and Computer Engineering, University of Toronto, 10 King's College Road, Toronto, Ontario M5S 3G4, Canada*
[2]*Advanced Technology, Materials and Research, Research and Development, Hoge Wei 33- Toyota Technical Centre, B-1930 Zaventem, Belgium*

(Received 5 August 2015; accepted 6 October 2015; published online 15 October 2015)

Atomic layer deposition (ALD), prized for its high-quality thin-film formation in the absence of high temperature or high vacuum, has become an industry standard for the large-area deposition of a wide array of oxide materials. Recently, it has shown promise in the formation of nanocrystalline sulfide films. Here, we demonstrate the viability of ALD lead sulfide for photodetection. Leveraging the conformal capabilities of ALD, we enhance the absorption without compromising the extraction efficiency in the absorbing layer by utilizing a ZnO nanowire electrode. The nanowires are first coated with a thin shunt-preventing TiO_2 layer, followed by an infrared-active ALD PbS layer for photosensing. The ALD PbS photodetector exhibits a peak responsivity of 10^{-2} A W^{-1} and a shot-derived specific detectivity of 3×10^9 Jones at 1530 nm wavelength. [http://dx.doi.org/10.1063/1.4933380]

Defined by its self-limiting and selectively reactive precursors, atomic layer deposition (ALD) is a versatile tool capable of forming high quality films of many materials. It is prized for its conformal film formation, low-temperature and pressure operation, uniformity over large areas, wide process window, and atomic thickness control.[1] For these reasons, it has become an industry standard for depositing thin-film oxides used in semiconductor devices. It has demonstrated compatibility with roll-to-roll processing.[2–4]

To complement the array of oxides capable of being deposited via ALD, researchers have demonstrated ALD of various sulfides. To date, there have been reports of 16 binary sulfide compounds made using ALD, a small fraction of the work done on ALD oxides.[5] Sulfides, unlike the conventional oxides deposited with ALD, have bandgaps extending far beyond the UV, through the visible and near infrared (IR), all the way out to the far-IR. Sulfide materials are used as the active medium in many semiconductor devices, including solar cells,[6] photodetectors,[7] light emitting diodes,[8] and lasers.[9]

Recently, ALD of PbS has been demonstrated.[10–15] PbS is a versatile direct-bandgap semiconductor with a large Bohr radius for excitons of 18 nm, resulting in a high degree of spectral tunability relative to its bulk bandgap, spanning all the way from 3000 nm to visible wavelengths, with tuning achieved via the quantum size effect.[16] Thin films of PbS grown with ALD are nanocrystalline, of high chemical purity, and exhibit bandgap control via quantum size tuning. Prior work on integrating an ALD PbS absorbing layer into an electronic device involved the growth of small quantum dots onto a mesoporous TiO_2 scaffold to harvest infrared solar light.[17]

We sought to use ALD PbS towards infrared photodetection. We first deposited ALD PbS onto a glass substrate to study its surface morphology. Using atomic force microscopy (Bruker PeakForce Tapping), we show that 300 cycles of ALD PbS forms nanocrystalline thin films (Figure 1(a)) with a grain size of 2 nm and arithmetic mean roughness of 2 nm. The thickness of this film was estimated to be 43 nm using a Dektak. We measured the linear absorption of this ALD PbS thin film to quantify the absorption coefficient. The absorption coefficient, α, exceeds 10^4 cm^{-1} below 1500 nm, highlighting its practical applications for short-wavelength-IR photodetection.[18]

We sought to utilize a ZnO electron-accepting electrode to form a heterojunction with our PbS active medium. However, we were unable to observe infrared photocurrent from ALD PbS/planar ZnO photodiodes. If the films are too thin, carriers can be extracted, but the device is absorption-limited. As the films are made thicker, extraction is compromised due to two effects: band misalignment at the ZnO and PbS interface, and the limited transport length in the nanocrystalline film.

To overcome this, we leveraged the conformal deposition capabilities of ALD and utilized a high aspect ratio electron-accepting nanostructured substrate—ZnO nanowires. This enabled us to increase the absorption of the films without extending the extraction length.

Figure 1(b) shows the absorption of ALD PbS films on nanowire and planar electrodes. These substrates were placed in the ALD side-by-side and exposed to the same deposition conditions. The film deposited on nanowires is much darker to the eye and absorbs significantly more light at all wavelengths. Figure 1(c) shows a high resolution transmission electron microscopy (HR-TEM) of a bare ZnO nanowire, and Figure 1(d) shows a nanowire coated with ALD PbS. The ALD PbS forms nanoislands which conformally coat the nanowire, consistent with prior reports.[14]

[a)]J. Xu and B. R. Sutherland contributed equally to this work.
[b)]Author to whom correspondence should be addressed. Electronic mail: ted.sargent@utoronto.ca

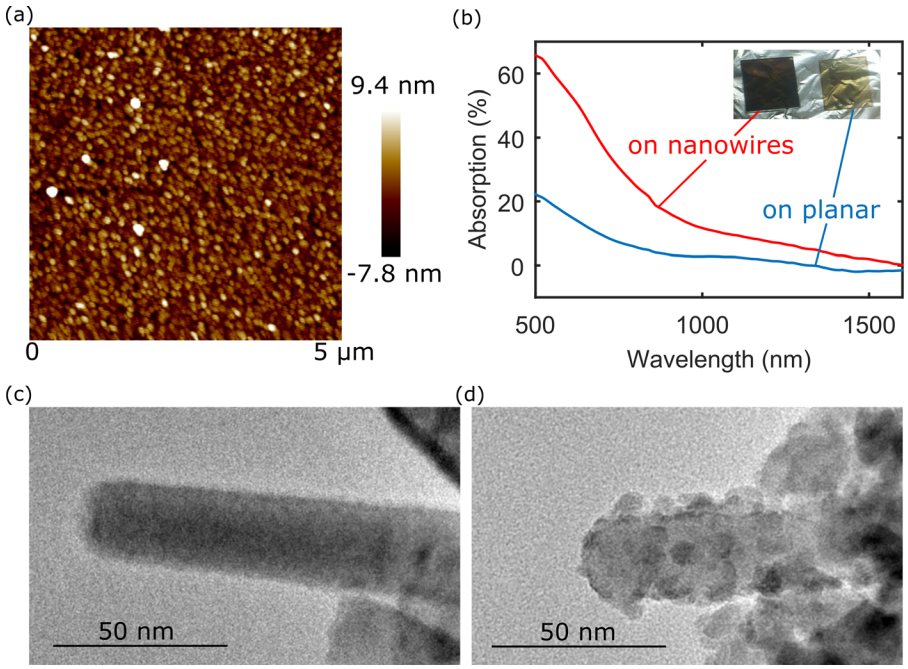

FIG. 1. ALD PbS material characterization on glass and growth of ALD PbS on nanowires. (a) Atomic force microscope image. Imaging the surface topology of 300 cycles of ALD PbS on glass reveals a nanocrystalline film with a grain size of 2 nm and an arithmetic mean roughness of 2 nm. (b) ALD PbS (60 cycles) absorption for two films deposited under identical conditions on two different substrates: ZnO nanowires (red), and on a planar ZnO layer (blue). (c) High resolution transmission electron microscopy (HR-TEM) of bare ZnO nanowires. (d) HR-TEM of ZnO nanowires coated with 60 cycles of ALD PbS. ALD PbS forms small nano-islands which conformally coat the nanowires.

To develop an ALD PbS short-wavelength infrared photodetector, we coated the nanowires first with a layer of ALD TiO_2 (20 cycles), followed by a thin film of an ALD PbS active layer (60 cycles).

The ALD TiO_2 interface layer was found to reduce shunt paths to the fluorine-doped tin oxide (FTO) substrate through the solution-processed ZnO layer.[18] In the absence of this layer, the dark current increases by over 4 orders of magnitude.[18] We measured the growth rate of ALD PbS on TiO_2 with ellipsometry to be approximately 1.1 Å/cycle.[18] TiO_2 on ZnO was found to have a growth rate of approximately 0.45 Å/cycle, corresponding to an approximately 1 nm coating on the nanowires.[18] By analyzing the TEM in Figure 1(d), we estimate the thickness of this layer to be on average 6 nm, corresponding to a growth rate of 1 Å/cycle which is consistent with the ellipsometry results.[18]

The nanostructured bottom electrode and absorbing layer are combined with a top spiro-OMeTAD (2,2′,7,7′-Tetrakis-(N,N-di-4-methoxyphenylamino)–9,9′-spirobifluorene) hole-transport layer and electrical contacts to form an IR-active heterojunction photodetector. The full device architecture is shown in Figure 2(a), with a corresponding cross-sectional SEM shown in Figure 2(b).

These devices were fabricated using the following procedure. Nanowires were grown on FTO substrates from a seed layer of ZnO deposited via spin-casting of a 5 mM zinc acetate solution and annealing for 20 min at 400 °C. The seed layer preferentially grows into nanowires during a vertical suspension of the film in a 90 °C aqueous solution of zinc nitrate hydrate and hexamethylenetetramine, each 0.025 M in concentration. The films were then dried in air for 4 h at 60 °C. These substrates were washed thoroughly with DI water, dried in air at 60 °C for 30 min, and then annealed at 450 °C for 2 h.

These samples were then transferred to the ALD reaction chamber (Cambridge Nanotech Savannah S100) at 150 °C with a nitrogen carrier gas at a volumetric flow rate of 10 sccm. First, a layer of TiO_2 was deposited from 20 ALD cycles of tetrakis-dimethyl-amido titanium (0.02 s pulse duration) and H_2O (0.015 s pulse duration) with a purge time of 20 s. Without breaking vacuum, we then deposited a thin film of PbS totaling 60 ALD cycles from lead bis(2,2,6,6-tetramethyl-3,5-heptanedionate) and H_2S. We used a pulse duration of 0.5 s for each precursor and a purge time of 20 s. To form the hole-transporting layer, Spiro-OMeTAD in chlorobenzene (63 mg/mL) was doped with *tert*-butylpyridine (20 μL/mL) and an acetonitrile solution (70 μL/mL) containing bis(trifluoromethane)sulfonimide lithium salt (170 mg/mL). This solution was spin-cast at 4000 rpm for 60 s in a glovebox containing dry air onto the

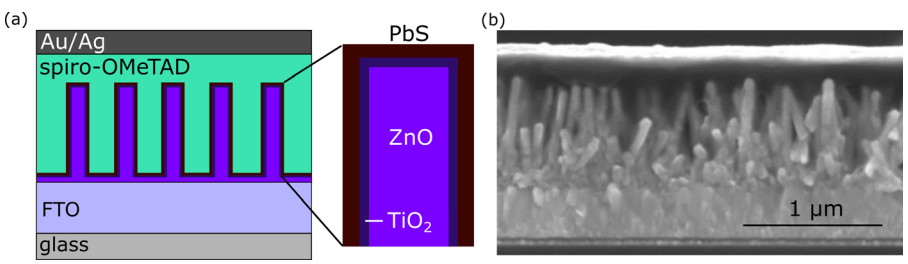

FIG. 2. Device architecture. (a) Device schematic. A thin adhesion layer of ALD TiO_2 is deposited onto self-assembled ZnO nanowire + FTO substrates. A thin layer of ALD PbS is then deposited, followed by a spiro-OMeTAD hole transport material and Au/Ag top contacts. (b) Device scanning electron microscopy image. 1 μm tall ZnO nanowires are grown, with good infiltration of Spiro into the nanowire network.

ALD PbS coated nanowire substrates after they had cooled down to room temperature. Electrical contacts were deposited through a shadow mask in an Angstrom Engineering Åmod thermal evaporation system inside an Innovative Technology glovebox. 50 nm of Au at a rate of 1.5 Å s^{-1} was deposited via electron-beam evaporation, and 100 nm of Ag at a rate of 2.0 Å s^{-1} was deposited via thermal evaporation. Each device is a circular pixel, 0.07 cm^2 in area as defined by the evaporation shadow mask.

We examined the double-pass linear absorption profile device with reference to the bare FTO + ZnO NW substrate.[18] The control device exhibits a sharp absorption onset at 350 nm wavelength, at the bandgap of ZnO. There is a broad tail extending into the IR, which is the IR-active component of the FTO. There is also a spectral feature at 1400 nm which is from the Li-doped Spiro-OMeTAD layer.[18] The device with ALD PbS shows significantly enhanced absorption out from 1600 nm, all the way down to 350 nm.

The current-voltage (JV) characteristic of this diode with and without the ALD TiO_2 interface layer is shown in Figure 3(a). We see that in the absence of the TiO_2 layer, the device exhibits soft-shorting behavior, marked by high dark current and poor rectification. The device with ALD PbS has a rectification ratio exceeding 1000 at ±1 V and a reverse saturation current density of 1 $\mu A\,cm^{-2}$ at −1 V. This device also exhibits a current minimum zero-bias offset, which is a feature of the TiO_2/Spiro junction.[18] We note that the inclusion of the ALD PbS layer reduces this effect, which we posit is a result of the reduced direct TiO_2/Spiro junction area. The TiO_2/Spiro interface also contributes no significant photocurrent, especially at infrared wavelengths. Despite this offset in the dark JV curve, we observe minimal hysteresis of a nanowire/ALD-PbS device under high-power broadband illumination (∼1 sun at AM1.5 G conditions).[18]

To measure responsivity accurately, we measured device photocurrent and dark current at a fixed bias in the steady-state, and not based on extrapolations from instantaneous JV curves. A sample steady-state on/off transient under 20 mW cm^{-2} 1530 nm illumination is shown in Figure 3(b). This illumination intensity is used for all remaining measurements at both wavelengths studied. Responsivity, given as the ratio of photocurrent to input power, is shown in Figure 3(b) as a function of reverse bias for both 1530 nm and 830 nm illumination sources. The ALD PbS photodiode achieves a peak responsivity at −6 V of 10^{-2} A W^{-1}.

The shot-derived specific detectivity is given in Figure 3(d). Shot noise, $I_{n,shot}$ is the noise associated with the discrete nature of electrons and is given by $(2qI_{dark}\Delta f)^{1/2}$, where q is the electronic charge constant, Δf the measurement bandwidth, and I_{dark} the dark current. Shot-derived specific detectivity, D^* is given as $R(A)^{1/2}/I_{n,shot}$, where R is the responsivity and A the device area. The ALD photodetector is most sensitive when operating at zero bias, achieving a specific detectivity of 8×10^9 and 3×10^9 Jones at 830 and 1530 nm, respectively. We have further supported these results with a direct measurement of the noise-current density and show that we approach within an order of magnitude of the shot-limit.[18] Commercially available photoconductive PbS detectors can achieve 7×10^{10} Jones at room temperature, but require the application of an external bias.[19] Colloidal PbS photodiodes have shown values in excess of 10^{13} Jones.[7,20,21] Our devices are currently limited by band alignment at the TiO_2/PbS interface, transport length through the nanocrystalline film, and absorption due to the ultra-thin active layer.

To overcome these issues, next steps for ALD PbS photodetectors include the development of tunable quantum well active layers. Engineering quantum-confined PbS active layers between ultra-thin barriers will enable control over the band alignment, pushing the electron affinity of the PbS

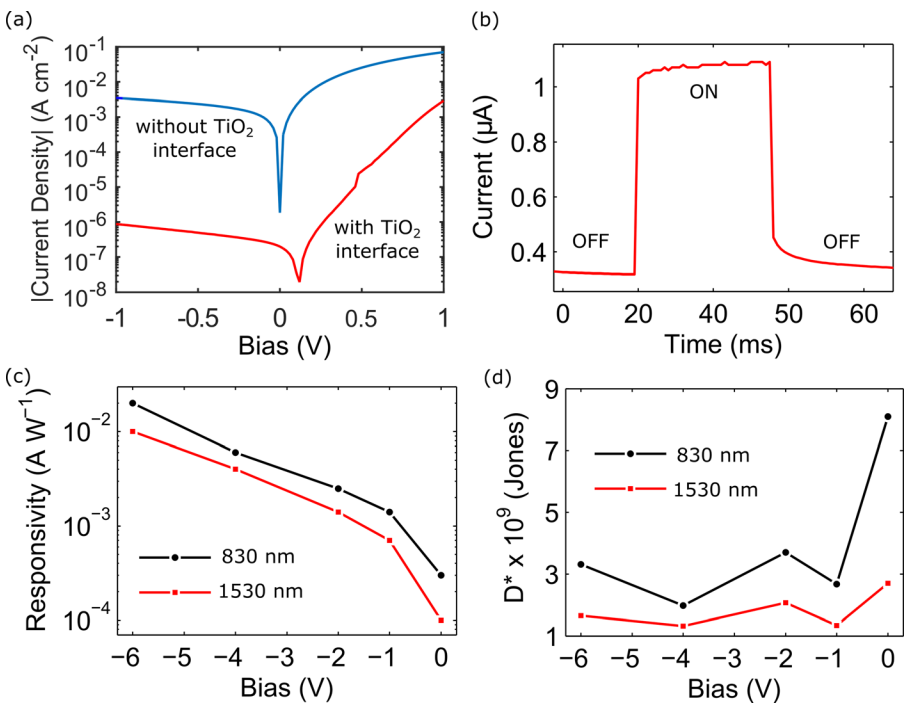

FIG. 3. Responsivity and specific detectivity at 20 mW cm^{-2} input illumination. (a) Dark current density vs. voltage characteristics for ALD PbS photodiodes with and without the ALD TiO_2 interface layer. (b) Sample photocurrent transient at 1530 nm, −1 V bias. (c) Bias dependent responsivity at 830 and 1530 nm. (d) Bias dependent shot-derived specific detectivity at 830 and 1530 nm.

towards that of TiO_2, consequently enabling thicker devices that can operate more efficiently at lower reverse biases, resulting in higher specific detectivity.

This works highlights the promise of atomic layer deposition for the formation of active media in semiconductor optoelectronic devices. Atomic layer deposition is a tool capable of much more than just oxide growth. It can form semiconductor active films capable of driving optoelectronic devices to be performance competitive with their epitaxial counterparts. Atomic layer deposition of lead sulfide is an excellent platform for not only infrared sensing, but for spectrally tunable optoelectronic devices broadly. Future work should be geared towards integrating lead sulfide quantum wells into these systems by utilizing the excellent thickness control of ALD, the wide bandgap tunability of PbS, and the capability of ALD to form ultrathin, pinhole-free, electron tunneling transparent oxide barriers.

The authors acknowledge funding by Toyota Motor Europe, and Ontario Research Fund—Research Excellence Program. The authors thank O. Voznyy, P. Kanjanaboos, and X. Lan for their help throughout the course of this study.

[1]S. M. George, Chem. Rev. **110**, 111 (2010).
[2]P. Poodt, A. Lankhorst, F. Roozeboom, K. Spee, D. Maas, and A. Vermeer, Adv. Mater. **22**, 3564 (2010).
[3]E. Dickey and W. A. Barrow, J. Vac. Sci. Technol. Vac. Surf. Films **30**, 021502 (2012).
[4]P. Poodt, D. C. Cameron, E. Dickey, S. M. George, V. Kuznetsov, G. N. Parsons, F. Roozeboom, G. Sundaram, and A. Vermeer, J. Vac. Sci. Technol. Vac. Surf. Films **30**, 010802 (2012).
[5]N. P. Dasgupta, X. Meng, J. W. Elam, and A. B. F. Martinson, Acc. Chem. Res. **48**, 341 (2015).
[6]A. H. Ip, S. M. Thon, S. Hoogland, O. Voznyy, D. Zhitomirsky, R. Debnath, L. Levina, L. R. Rollny, G. H. Carey, A. Fischer, K. W. Kemp, I. J. Kramer, Z. Ning, A. J. Labelle, K. W. Chou, A. Amassian, and E. H. Sargent, Nat. Nanotechnol. **7**, 577 (2012).
[7]J. P. Clifford, G. Konstantatos, K. W. Johnston, S. Hoogland, L. Levina, and E. H. Sargent, Nat. Nanotechnol. **4**, 40 (2009).
[8]X. Dai, Z. Zhang, Y. Jin, Y. Niu, H. Cao, X. Liang, L. Chen, J. Wang, and X. Peng, Nature **515**, 96 (2014).
[9]C. Dang, J. Lee, C. Breen, J. S. Steckel, S. Coe-Sullivan, and A. Nurmikko, Nat. Nanotechnol. **7**, 335 (2012).
[10]N. P. Dasgupta, S. P. Walch, and F. Prinz, ECS Trans. **16**, 29 (2008).
[11]N. P. Dasgupta, W. Lee, and F. B. Prinz, Chem. Mater. **21**, 3973 (2009).
[12]W. Lee, N. P. Dasgupta, H. J. Jung, J.-R. Lee, R. Sinclair, and F. B. Prinz, Nanotechnology **21**, 485402 (2010).
[13]W. Lee, N. P. Dasgupta, O. Trejo, J.-R. Lee, J. Hwang, T. Usui, and F. B. Prinz, Langmuir **26**, 6845 (2010).
[14]N. P. Dasgupta, H. J. Jung, O. Trejo, M. T. McDowell, A. Hryciw, M. Brongersma, R. Sinclair, and F. B. Prinz, Nano Lett. **11**, 934 (2011).
[15]B. R. Sutherland, S. Hoogland, M. M. Adachi, P. Kanjanaboos, C. T. O. Wong, J. J. McDowell, J. Xu, O. Voznyy, Z. Ning, A. J. Houtepen, and E. H. Sargent, Adv. Mater. **27**, 53 (2015).
[16]F. W. Wise, Acc. Chem. Res. **33**, 773 (2000).
[17]T. P. Brennan, O. Trejo, K. E. Roelofs, J. Xu, F. B. Prinz, and S. F. Bent, J. Mater. Chem. A **1**, 7566 (2013).
[18]See supplementary material at http://dx.doi.org/10.1063/1.4933380 for absorption coefficient, spatial band diagram and effect of TiO_2 layer, thickness measurements, device absorption, spiro parasitic absorption, AM 1.5 characterization with and without ALD PbS, AM 1.5 hysteresis-free current-voltage sweep, and direct measurement of noise current.
[19]P. R. Griffiths and J. A. De Haseth, *Fourier Transform Infrared Spectrometry*, 2nd ed. (Wiley, 2007).
[20]B. N. Pal, I. Robel, A. Mohite, R. Laocharoensuk, D. J. Werder, and V. I. Klimov, Adv. Funct. Mater. **22**, 1741 (2012).
[21]J. Y. Kim, V. Adinolfi, B. R. Sutherland, O. Voznyy, S. J. Kwon, T. W. Kim, J. Kim, H. Ihee, K. Kemp, M. Adachi, M. Yuan, I. Kramer, D. Zhitomirsky, S. Hoogland, and E. H. Sargent, Nat. Commun. **6**, 7772 (2015).